INTERNATIONAL STANDARD

ISO 15901-2

Second edition
2022-01

Pore size distribution and porosity of solid materials by mercury porosimetry and gas adsorption —

Part 2: Analysis of nanopores by gas adsorption

Distribution des dimensions des pores et porosité des matériaux solides par porosimétrie au mercure et par adsorption de gaz —
Partie 2: Analyse des nanopores par adsorption de gaz

Reference number
ISO 15901-2:2022(E)

COPYRIGHT PROTECTED DOCUMENT

ISO copyright office
CP 401 • Ch. de Blandonnet 8
CH-1214 Vernier, Geneva
Phone: +41 22 749 01 11
Email: copyright@iso.org
Website: www.iso.org

Published in Switzerland

Contents

Page

Foreword

ISO (the International Organization for Standardization) is a worldwide federation of national standards bodies (ISO member bodies). The work of preparing International Standards is normally carried out through ISO technical committees. Each member body interested in a subject for which a technical committee has been established has the right to be represented on that committee. International organizations, governmental and non-governmental, in liaison with ISO, also take part in the work. ISO collaborates closely with the International Electrotechnical Commission (IEC) on all matters of electrotechnical standardization.

The procedures used to develop this document and those intended for its further maintenance are described in the ISO/IEC Directives, Part 1. In particular, the different approval criteria needed for the different types of ISO documents should be noted. This document was drafted in accordance with the editorial rules of the ISO/IEC Directives, Part 2 (see www.iso.org/directives).

Attention is drawn to the possibility that some of the elements of this document may be the subject of patent rights. ISO shall not be held responsible for identifying any or all such patent rights. Details of any patent rights identified during the development of the document will be in the Introduction and/or on the ISO list of patent declarations received (see www.iso.org/patents).

Any trade name used in this document is information given for the convenience of users and does not constitute an endorsement.

For an explanation of the voluntary nature of standards, the meaning of ISO specific terms and expressions related to conformity assessment, as well as information about ISO's adherence to the World Trade Organization (WTO) principles in the Technical Barriers to Trade (TBT), see www.iso.org/iso/foreword.html.

This document was prepared by Technical Committee ISO/TC 24, *Particle characterization including sieving*, Subcommittee SC 4, *Particle characterization*.

This second edition cancels and replaces ISO 15901-2:2006 and ISO 15901-3:2007, which have been technically revised. It also incorporates the Technical Corrigendum ISO 15901-2:2006/Cor.1:2007.

The main changes compared to the previous edition are as follows:

— the analysis of nanopores by gas adsorption which combines the characterization of both micro- and mesopores is now addressed;

— the classification of adsorption isotherms and hysteresis loops has been updated.

A list of all parts in the ISO 15901 series can be found on the ISO website.

Any feedback or questions on this document should be directed to the user's national standards body. A complete listing of these bodies can be found at www.iso.org/members.html.

Introduction

In general, different types of pores may be pictured as apertures, channels, or cavities within a solid body or as the space (i.e. interstices or voids) between solid particles in a bed, compact or aggregate. Porosity is a term which is often used to indicate the porous nature of solid material and is more precisely defined as the ratio of the volume of accessible pores and voids to the total volume occupied by a given amount of the solid. According to the 2015 IUPAC recommendations[1], nanopores are defined as pores with internal widths of equal or less than 100 nm and are divided into several subgroups dependent on their pore width:

— pores with width greater than about 50 nm are called macropores;

— pores of widths between 2 nm and 50 nm are called mesopores;

— pores with width of about 2 nm and less are called micropores;

Further, IUPAC suggested a subclassification of micropores into supermicropores (pore width 0,7 nm to 2 nm), and ultramicropores (pore width < 0,7 nm). In addition to the accessible pores, a solid may contain closed pores which are isolated from the external surface and into which fluids are not able to penetrate. The characterization of closed pores, i.e. cavities with no access to an external surface, is not covered in this document.

Porous materials may take the form of fine or coarse powders, compacts, extrudates, sheets or monoliths. Their characterization usually involves the determination of the pore size distribution as well as the total pore volume or porosity. For some purposes it is also necessary to study the pore shape and interconnectivity, and to determine the internal and external surface area.

Porous materials have great technological importance, e.g. in the context of the following:

a) controlled drug release;

b) catalysis;

c) gas separation;

d) filtration including sterilization;

e) materials technology;

f) environmental protection and pollution control;

g) natural reservoir rocks;

h) building material properties;

i) polymer and ceramic industries.

It is well established that the performance of a porous solid (e.g. its strength, reactivity, permeability or adsorbent power) is dependent on its pore structure. Many different methods have been developed for the characterization of pore structure. The choice of the most appropriate method depends on the application of the porous solid, its chemical and physical nature and the range of pore size.

Different methods for the characterization of nanopores are available, including spectroscopy, electron and tunnel microscopy and sorption methods. In view of the complexity of most porous solids, it is not surprising that the results obtained are not always in agreement and that no single technique can be relied upon to provide a complete picture of the pore structure. Among these, mercury porosimetry (see ISO 15901-1) and gas adsorption are popular ones because by combining both it is possible to assess a wide range of pore sizes from below 0,5 nm up to 400 µm. While mercury porosimetry is the standard technique for macropore analysis, gas adsorption techniques allow to assess pores up to approximately 100 nm. In this case, physical adsorption can be conveniently used, is not destructive, and is not that cost intensive as compared to some of the above-mentioned methods. Particularly, with regard to the

application of microporous material as specific sorbents, molecular sieves and carriers for catalysts and biological active material, the field-proven methods of gas sorption are of special value.

The measuring techniques of the method described in this document are similar to those described in ISO 9277 for the measurement of gas adsorption at low temperature. However, in order to assess the full range of pore sizes including microporosity, adsorption experiments have to be performed over a wide range of pressures from the ultralow pressure range (e.g. turbomolecular pump vacuum) up to atmospheric pressure (0,1 MPa).

Pore size distribution and porosity of solid materials by mercury porosimetry and gas adsorption —

Part 2:
Analysis of nanopores by gas adsorption

1 Scope

This document describes a method for the evaluation of porosity and pore size distribution by physical adsorption (or physisorption). The method is limited to the determination of the quantity of a gas adsorbed per unit mass of sample as a function of pressure at a controlled, constant temperature[1]-[9]. Commonly used adsorptive gases for physical adsorption characterization include nitrogen, argon, krypton at the temperatures of liquid nitrogen and argon (77 K and 87 K respectively) as well as CO_2 (at 273 K). Traditionally, nitrogen and argon adsorption at 77 K and 87 K, respectively, allows one to assess pores in the approximate range of widths 0,45 nm to 50 nm, although improvements in temperature control and pressure measurement allow larger pore widths to be evaluated. CO_2 adsorption at 273 K – 293 K can be applied for the microporous carbon materials exhibiting ultramicropores. Krypton adsorption at 77 K and 87 K is used to determine the surface area or porosity of materials with small surface area or for the analysis of thin porous films.

The method described is suitable for a wide range of porous materials. This document focuses on the determination of pore size distribution from as low as 0,4 nm up to approximately 100 nm. The determination of surface area is described in ISO 9277. The procedures which have been devised for the determination of the amount of gas adsorbed may be divided into two groups:

— those which depend on the measurement of the amount of gas removed from the gas phase, i.e. manometric (volumetric) methods;

— those which involve the measurement of the uptake of the gas by the adsorbent (i.e. direct determination of increase in mass by gravimetric methods).

In practice, static or dynamic techniques can be used to determine the amount of gas adsorbed. However, the static manometric method is generally considered the most suitable technique for undertaking physisorption measurements with nitrogen, argon and krypton at cryogenic temperatures (i.e. 77 K and 87 K, the boiling temperature of nitrogen and argon, respectively) with the goal of obtaining pore volume and pore size information. This document focuses only on the application of the manometric method.

2 Normative references

The following documents are referred to in the text in such a way that some or all of their content constitutes requirements of this document. For dated references, only the edition cited applies. For undated references, the latest edition of the referenced document (including any amendments) applies.

ISO 3165, *Sampling of chemical products for industrial use — Safety in sampling*

ISO 8213, *Chemical products for industrial use — Sampling techniques — Solid chemical products in the form of particles varying from powders to coarse lumps*

ISO 9277, *Determination of the specific surface area of solids by gas adsorption — BET method*

ISO 14488, *Particulate materials — Sampling and sample splitting for the determination of particulate properties*

3 Terms and definitions

For the purposes of this document, the following terms and definitions apply.

ISO and IEC maintain terminological databases for use in standardization at the following addresses:

— ISO Online browsing platform: available at https://www.iso.org/obp

— IEC Electropedia: available at https://www.electropedia.org/

3.1
adsorbate
adsorbed gas

3.2
adsorption
enrichment of the adsorptive at the external and accessible internal surfaces of a solid

3.3
adsorptive
gas or vapour to be adsorbed

3.4
adsorbent
solid material on which adsorption occurs

3.5
adsorption isotherm
relationship between the amount of gas adsorbed and the equilibrium pressure of the gas at constant temperature

3.6
adsorbed amount
amount of gas adsorbed at a given pressure, p, and temperature, T

3.7
equilibrium adsorption pressure
pressure of the adsorptive in equilibrium with the adsorbate

3.8
monolayer amount
amount of the adsorbate that forms a monomolecular layer over the surface of the adsorbent

3.9
monolayer capacity
volumetric equivalent of monolayer amount expressed as gas at standard conditions of temperature and pressure (STP)

3.10
nanopore
pore with width of 100 nm or less

3.11
macropore
pore with width greater than about 50 nm

3.12
mesopore
pore with width between approximately 2 nm and 50 nm

3.13
micropore
pore with width of about 2 nm or less

3.14
supermicropore
pore with width between approximately 0,7 nm and 2 nm

3.15
ultramicropore
pore with width of approximately < 0,7 nm

3.16
physisorption
weak bonding of the adsorbate, reversible by small changes in pressure or temperature

3.17
pore size
pore width, i.e. diameter of cylindrical pore or distance between opposite walls of slit

3.18
pore volume
volume of pores as determined by stated method

3.19
relative pressure
ratio of the equilibrium adsorption pressure, p, to the saturation vapour pressure, p_0, at analysis temperature

3.20
saturation vapour pressure
vapour pressure of the bulk liquefied adsorptive at the temperature of adsorption

3.21
volume adsorbed
volumetric equivalent of the amount adsorbed, expressed as gas at standard conditions of temperature and pressure (STP), or expressed as the adsorbed liquid volume of the adsorbate

4 Symbols

For the purposes of this document, the following symbols apply, together with their units. All specific dimensions are related to sample mass, in grams.

Symbol	Description	Unit
A_a	Kirkwood-Mueller constant of adsorptive	$J \cdot cm^6$
A_s	Kirkwood-Mueller constant of adsorbent	$J \cdot cm^6$
a_s	specific surface area	$m^2 \cdot g^{-1}$
$a_{s,ref}$	specific surface area of reference sample	$m^2 \cdot g^{-1}$
α_a	polarizability of adsorptive	cm^3
α_s	normalized adsorption	1[a]
α_{s*}	polarizability of adsorbent	cm^3
c	speed of light	$m \cdot s^{-1}$
d_a	diameter of an adsorptive molecule	nm
d_{HS}	diameter of hard spheres	nm

[a] According to ISO 80000-1, the coherent SI unit for any quantity of dimension one (at present commonly determined "dimensionless") is the unit one, symbol 1.

Symbol	Description	Unit
d_p	pore diameter (cylindrical pore)	nm
d_s	diameter of an adsorbent molecule	nm
d_0	$d_0 = (d_s + d_a)/2$, distance between adsorptive and adsorbent molecules	nm
ε_{ff}/k_B	well depth parameter of gas-gas Lennard Jones potential	K
ε_{sf}/k_B	well depth parameter of gas-solid Lennard Jones potential	K
k_B	Boltzmann constant (1,381 × 10^{-23})	J K^{-1}
l	nuclei-nuclei pore width	nm
$m_a{}^*$	mass adsorbed	g
m_e	mass of an electron	kg
N_A	Avogadro's constant (6,022 × 10^{23})	mol^{-1}
N_a	number of atoms per unit area (m^2) of monolayer	m^{-2}
N_s	number of atoms per unit area (m^2) of adsorbent	m^{-2}
n_a	specific amount adsorbed	$mol \cdot g^{-1}$
P	pressure of the adsorptive in equilibrium with the adsorbate	Pa
p_0	saturation vapour pressure of the adsorptive	Pa
p/p_0	relative pressure of the adsorptive	1[a]
R	ideal gas constant (8,314)	$Jmol^{-1}K^{-1}$
ρ_g	gas density	$g \cdot cm^{-3}$
$\rho_{g,STP}$	gas density at STP (273,15 K; 101,3 kPa)	$g \cdot cm^{-3}$
ρ_l	liquid density	$g \cdot cm^{-3}$
σ	distance between two molecules at zero interaction energy	nm
σ_{ff}	distance parameter of gas-gas Lennard Jones potential	nm
σ_{sf}	distance parameter of gas-solid Lennard Jones potential	nm
T	temperature	K
T_{cr}	critical temperature	K
t	statistical layer thickness	nm
V_a	specific volume of the adsorbate	$cm^3 \cdot g^{-1}$
V_g	specific adsorbed gas volume at STP (273,15 K; 101,3 kPa)	$cm^3 \cdot g^{-1}$
V_{micro}	micropore volume	$cm^3 \cdot g^{-1}$
W	pore width (slit pore)	nm
χ_a	diamagnetic susceptibility of adsorptive	cm^3
χ_s	diamagnetic susceptibility of adsorbent	cm^3

[a] According to ISO 80000-1, the coherent SI unit for any quantity of dimension one (at present commonly determined "dimensionless") is the unit one, symbol 1.

5 Principles

5.1 General

Physisorption is a general phenomenon and occurs whenever an adsorbable gas (the adsorptive) is brought into contact with the surface of a solid (the adsorbent). The forces involved are the van der Waals forces. Physisorption in porous materials is governed by the interplay between the strength of fluid-wall and fluid-fluid interactions as well as the effects of confined pore space on the state of fluids in narrow pores. The effect of pore width on the interaction potential is demonstrated schematically in Figure 1[8].

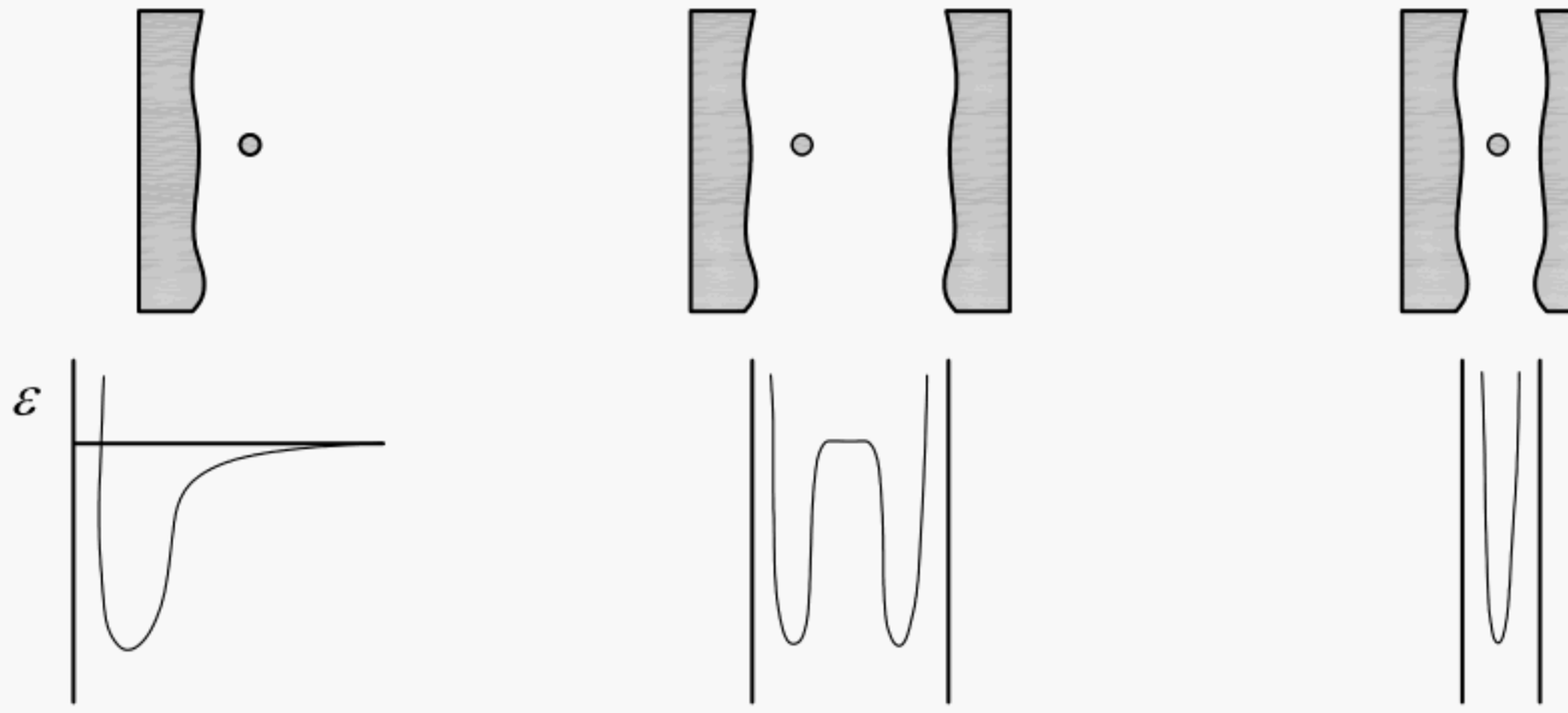

Figure 1 — Schematic illustration of adsorption potential, ε, on (a) planar, nonporous surface; (b) mesopore; (c) micropore

The interplay between the strength of attractive adsorptive-adsorbent interactions and the effect of confinement (as controlled by pore size/geometry) affect the shape of adsorption isotherm, as demonstrated in the IUPAC classification of adsorption isotherms[1] as shown in Figure 2.

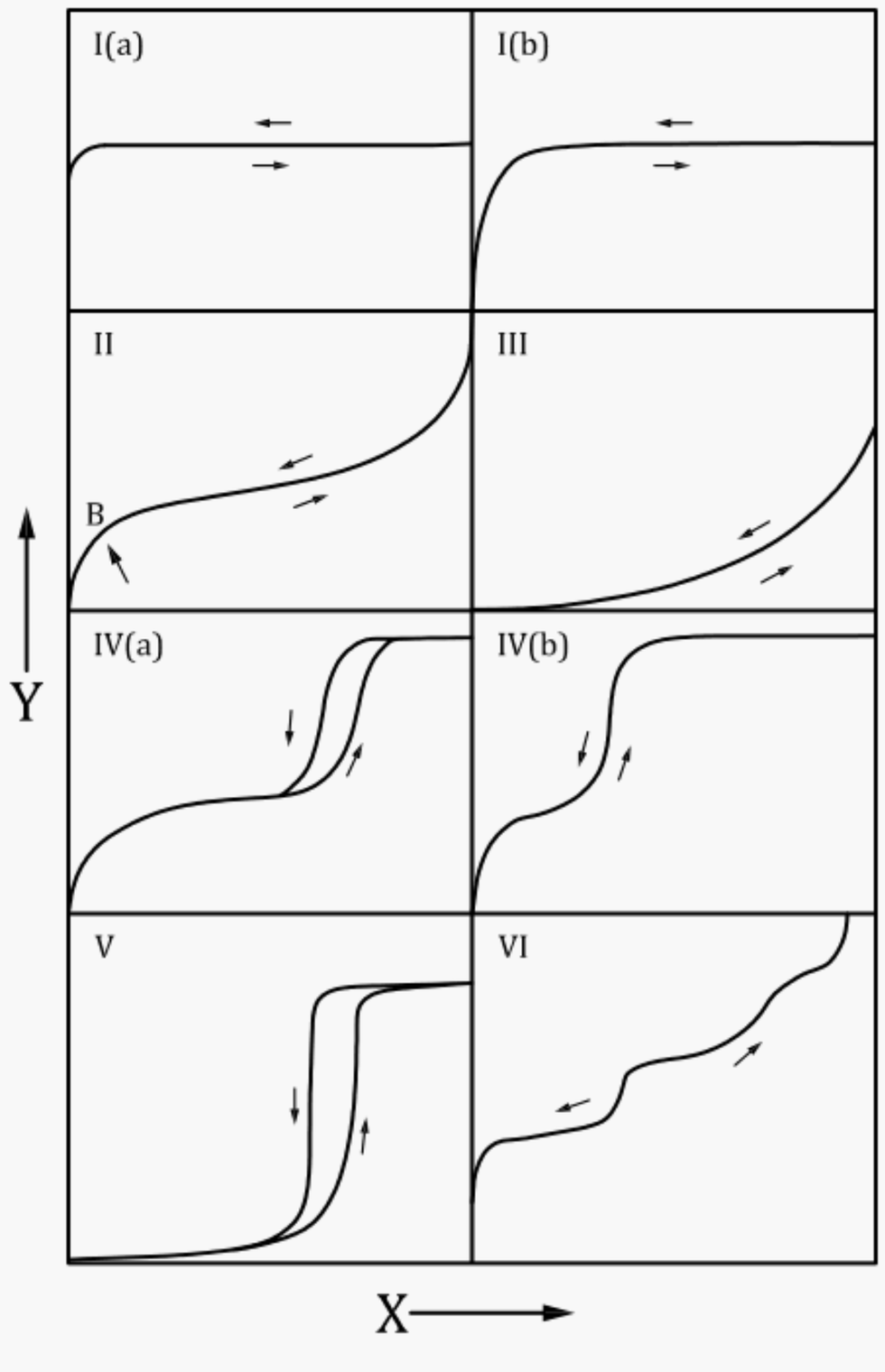

Key

X relative pressure

Y amount adsorbed

Figure 2 — Standard isotherm types (IUPAC 2015)

Reversible Type I isotherms are given by microporous solids having relatively small external surfaces (e.g. some activated carbons, molecular sieve zeolites and certain porous oxides). Because the pore size is similar to the molecule diameter, the choice of the gas is decisive, i.e. the size of the gas molecule controls the accessibility of the pores, and hence affects the obtained porosity information. A Type I isotherm is concave to the relative pressure (i.e. p/p_0 axis) and the amount adsorbed approaches a limiting value. This limiting uptake is governed by the accessible micropore volume rather than by the internal surface area. A steep uptake at very low p/p_0 is due to enhanced adsorbent-adsorptive interactions in narrow micropores (micropores of molecular dimensions), resulting in micropore filling at very low p/p_0. Type I(a) isotherms are given by microporous materials having mainly narrow micropores (of width ≤ 1 nm), which includes ultramicropores). A significant portion of the micropores is indicated by a large and steep increase of the isotherm near its origin and subsequent bending to a plateau. Type I(b) isotherms are found with materials having pore size distributions over a broader range including wider micropores (including supermicropores).

Type II isotherms are typically produced by solids which are non-porous or macroporous. Point B is often taken as indicative of the completion of the monolayer capacity.

Type III isotherms are distinguished by a convexity towards the relative pressure axis. These isotherms are found when weak gas-solid interactions occur on non-porous or macroporous solids (e.g. water adsorption on carbon surfaces).

Type IV isotherms are found for mesoporous solids. Type IV isotherms are given by mesoporous adsorbents (e.g. many oxide gels, industrial adsorbents and mesoporous molecular sieves). The

adsorption behaviour in mesopores is determined by the adsorbent-adsorptive interactions and by the interactions between the molecules in the condensed state. In this case, the initial monolayer-multilayer adsorption on the mesopore walls, which takes the same path as the corresponding part of a Type II isotherm, is followed by pore condensation. Pore condensation is the phenomenon whereby a gas condenses to a liquid-like phase in a pore at a pressure p less than the saturation pressure p_0 of the bulk liquid. This leads to the appearance of a Type IV adsorption isotherm. A typical feature of Type IV isotherms is a final saturation plateau, of variable length (sometimes reduced to a mere inflexion point).

In the case of a Type IV(a) isotherm, capillary condensation is accompanied by hysteresis. This occurs when the pore width exceeds a certain critical width, which is dependent on the adsorption system and temperature (e.g. for nitrogen and argon adsorption in cylindrical pores at 77 K and 87 K, respectively, hysteresis starts to occur for pores wider than ~ 4 nm). With adsorbents having mesopores of smaller width, completely reversible Type IV(b) isotherms are observed. In principle, Type IV(b) isotherms are also given by conical and cylindrical mesopores that are closed at the tapered end.

Type V isotherms are characterized by a convexity to the relative pressure axis. Unlike Type III isotherms there occurs a point of inflection at higher relative pressures. Type V isotherms result from weak gas-solid interactions on microporous and mesoporous solids (e.g. water adsorption on micro-or mesoporous carbons).

Type VI isotherms are notable for the step-like nature of the sorption process. The steps result from sequential multilayer adsorption or uniform non-porous surfaces. Amongst the best examples of Type VI isotherms are those obtained with argon or krypton at low temperature on graphitized carbon blacks.

There are various phenomena which contribute to the occurrence of hysteresis, and this is also reflected in the IUPAC classification of hysteresis loops[1] shown in Figure 3.

Type H1 hysteresis loops are observed for mesoporous materials with relatively narrow pore size distributions as for instance in ordered mesoporous silicas (e.g. MCM-41, MCM-48, SBA-15), some controlled pore glasses and ordered, mesoporous carbons, and materials with mesoporous cylindrical pores and for agglomerates of spheroidal particles of uniform size. Usually, network effects are minimal and occurrence of Type H1 hysteresis is often a clear sign that hysteresis is entirely caused by delayed condensation, i.e. a metastable adsorption branch.

Hysteresis loops of Type H2 are given by more complex pore structures in which network effects are important[10]. The very steep desorption branch, which is a characteristic feature of H2(a) loops, can be attributed either to pore-blocking/percolation in a narrow range of pore necks or to cavitation-induced evaporation, as well as for some 2-dimensional materials with slit-shaped pores. H2(a) loops are for instance given by many silica gels, some porous glasses (e.g. vycor) as well as some ordered mesoporous materials (e.g. SBA-16 and KIT-5 silicas). The Type H2(b) loop is also associated with pore blocking, but the size distribution of neck widths is now much larger. Examples of this type of hysteresis loops have been observed with mesocellular silica foams and certain mesoporous ordered silicas after hydrothermal treatment.

A distinctive feature of Type H3 is that the lower limit of the desorption branch is normally located at the cavitation-induced p/p_0. Loops of this type are given for instance by non-rigid aggregates of plate-like particles (e.g. certain clays), but also if the pore network consists of macropores which are not completely filled with pore condensate. Capillary condensation between small particles can also lead to Type H3 hysteresis.

Hysteresis of Type H4 is somewhat similar to Type H3, but the adsorption branch shows a more pronounced uptake at low p/p_0 being associated with the filling of micropores. H4 loops are often found with aggregated crystals of zeolites, some mesoporous zeolites, and micro-mesoporous carbons.

Type H5 hysteresis has a distinctive form associated with certain pore structures containing both open and partially blocked mesopores (e.g. plugged hexagonal templated silicas). Over an appreciable range, the isotherm shape is very similar to that of H4, but there is now a well-defined plateau at high p/p_0.

As already indicated, the common feature of H3, H4 and H5 loops is the sharp step-down of the desorption branch, indicative of cavitation induced evaporation. Generally, this is located in a narrow

range of p/p_0 for the particular adsorptive and temperature (e.g. at $p/p_0 \sim 0{,}4 - 0{,}5$ for nitrogen at temperatures of 77 K)[10].

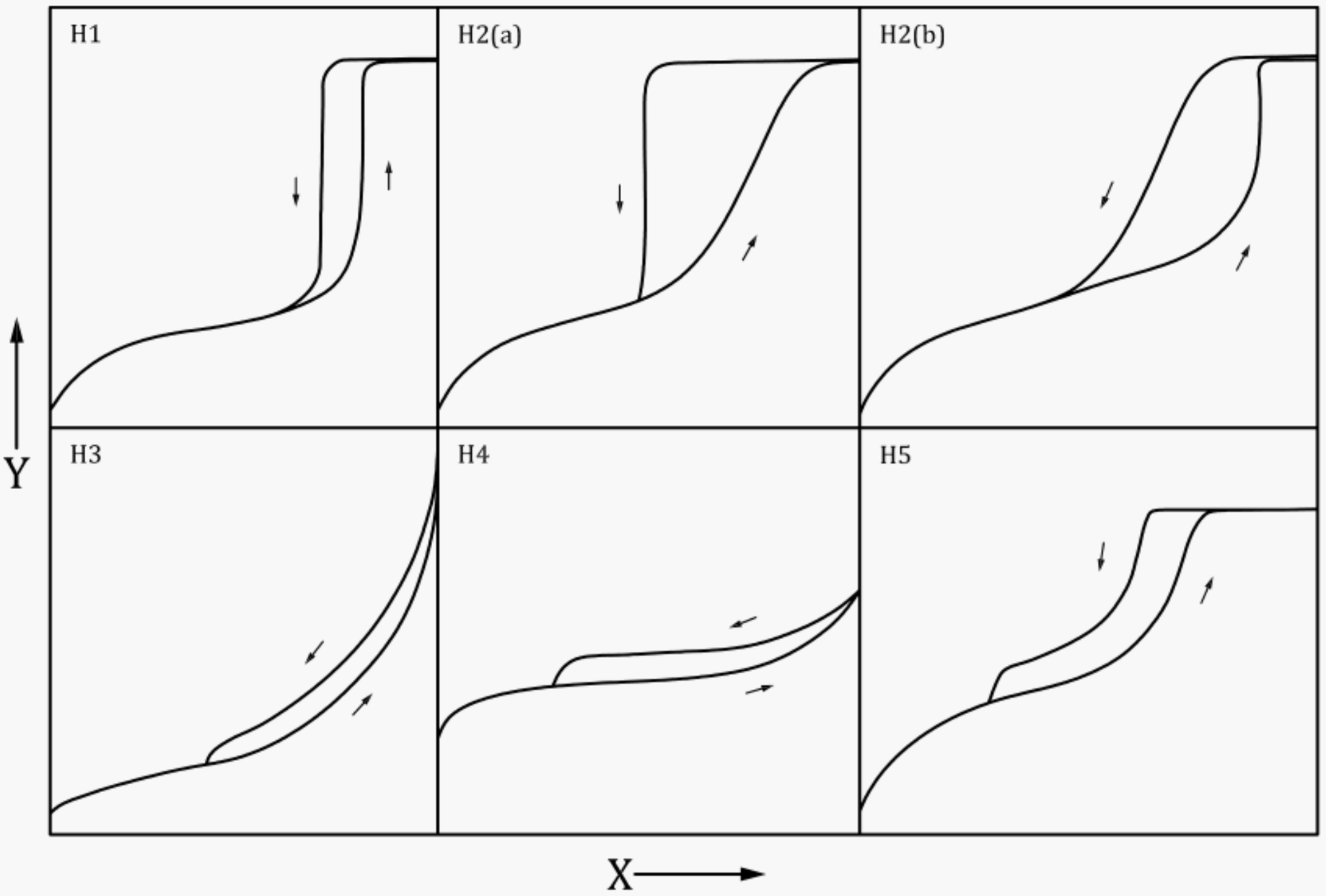

Key

X relative pressure

Y amount adsorbed

Figure 3 — Standard types of hysteresis loop (IUPAC 2015)

5.2 Methods of measurement

The experimental data required to establish an adsorption/desorption (sorption) isotherm may be obtained by volumetric (manometric) or gravimetric methods, by measurements either at stepwise, varied pressure with observation of the equilibrium value of pressure or mass, respectively, or at a continuously varied pressure. Because adsorption/desorption equilibrium can take a long time, the stepwise manometric method is recommended to ensure the measurement of equilibrium values.

The manometric (volumetric) method is based on calibrated volumes and pressure measurements (see ISO 9277). The volume adsorbed is calculated as the difference between the quantity of gas admitted and the quantity of gas filling the void volume (free space in the sample container including connections) by application of the general gas equation. Equilibrium is observed by monitoring the pressure in the free space. It is necessary to take special care in the pressure measurements for micropores as physical adsorption occurs at relative pressures substantially lower than in the case of sorption phenomena in mesopores and can span a broad spectrum of pressures (up to seven orders of magnitude in pressure). Consequently, contrary to the situation for mesopore measurements (pores fill here at relative pressures greater than approximately 0,15 for nitrogen and argon adsorption at 77 K and 87 K, respectively) more than one pressure transducer is necessary to measure the equilibrium pressure with sufficient accuracy. In order to study the adsorption of gases like nitrogen and argon (at their boiling temperatures) within a relative pressure range of $10^{-7} < p/p_0 < 1$ with sufficiently high accuracy, it is desirable to use a combination of different transducers with maximum ranges of 0,133 kPa (1 Torr[1)]), 1,33 kPa (10 Torr) and 133 kPa (1 000 Torr). In addition, one needs to ensure

1) Torr is a deprecated unit.

that the sample cell and the manifold can be evacuated to pressures as low as possible, which requires a proper high-vacuum pumping system. The desired low pressure can be achieved by using a turbomolecular pump. For gas pressures below about 1,3 Pa (i.e. $p/p_0 < 10^{-5}$ for nitrogen and argon adsorption at 77 K and 87 K, respectively), it is necessary to take into account the pressure differences along the capillary of the sample bulb caused by the Knudsen effect (i.e. one needs to apply a correction for thermal transpiration).

Care shall also be taken to properly select the equilibration conditions. Too short of an equilibration time may lead to under-equilibrated data and isotherms shifted to too high relative pressures. Under-equilibration is often an issue in the very low relative pressure region of the isotherm, since equilibration in narrow micropores tends to be very slow. For highest accuracy the saturation pressure p_0 should be recorded for every data point (by means of a dedicated saturation pressure transducer), i.e. this is most important for providing acceptable accuracy in the measurement of p/p_0 at high pressures, which is particularly important for evaluation of the size distribution of larger mesopores.

5.3 Choice of adsorptive

The proper choice of adsorptive is also crucial for an accurate and comprehensive pore structural analysis. For many years, nitrogen adsorption at 77 K has been generally accepted as the standard method for both micropore and mesopore size analysis, but for several reasons it has become evident that nitrogen is not a good choice for assessing the micropore size distribution. It is well known that the quadrupole of the nitrogen molecule is largely responsible for the specific interaction with a variety of surface functional groups and exposed ions. This not only affects the orientation of the adsorbed nitrogen molecule on the adsorbent surface [which will affect the reliability of applying the Brunauer-Emmett-Teller (BET) method for surface area analysis[1]], but it also strongly affects the micropore filling pressure. For example, for many zeolites and metal-organic frameworks (MOFs), the initial stage of physisorption is shifted to extremely low pressures (to ~10^{-7}) where the rate of diffusion is extremely slow, making it difficult to measure equilibrated adsorption isotherms. Specific interactions with surface functional groups cause the problem that the pore filling pressure is not correlated with the pore size in a straightforward way. In contrast to nitrogen at 77 K argon at 87 K (liquid argon temperature) does not exhibit specific interactions with surface functional groups. As a consequence of this and the slightly higher temperature, argon at 87 K fills micropores of dimensions between 0,5 nm and 1 nm at significantly higher relative pressures compared to nitrogen at 77 K, leading to accelerated diffusion and faster equilibration time. The pore filling pressure of argon (87 K) is often shifted 1 to 1,5 decades in relative pressure as compared to nitrogen. Hence, argon adsorption at 87 K allows one to obtain high resolution adsorption isotherms in order to resolve small differences in texture; in fact, such argon (87 K) isotherms can be considered a fingerprint of the pore structure. Hence, it is beneficial to analyse microporous materials by using argon as the adsorptive at 87 K[1]. However, if one is only interested in the determination of mesoporosity nitrogen adsorption at 77 K will give satisfactory results (the effect of quadrupole interactions is more severe for filling of micropore at ultralow pressures), although even for mesopore analysis argon adsorption at 87 K is preferable because of higher sensitivity in detecting small amounts of mesoporosity.

Despite the advantages which argon adsorption at 87 K offers, there exists the well-known problem of restricted diffusion in various ultramicroporous carbon materials, which prevents nitrogen and also argon molecules from entering the narrowest micropores – pores of width < 0,45 nm. Here it is advantageous to use CO_2 as adsorptive at 273,15 K. The saturation pressure at this temperature is about 3,48 MPa, i.e. in order to achieve the small relative pressures required to monitor the micropore filling, a turbomolecular pump-level vacuum is not necessary. At these relatively high temperatures and pressures, significant diffusion limitations no longer exist, which leads to the situation that equilibrium is achieved much faster relative to low-temperature nitrogen and argon experiments. It is therefore possible to reliably assess pores as small as 0,4 nm. With CO_2 adsorption up to 101,3 kPa (1 atm), one can detect pores from the narrowest micropores up to about 1 nm.

6 Measurement procedure

6.1 Sampling

Sampling shall be performed in accordance with ISO 3165, ISO 8213, and ISO 14488. The sample for test shall be representative of the bulk material and should be of an appropriate quantity. Repeated measurements using a second sample are recommended.

6.2 Sample pretreatment

The sample should be degassed in vacuum better than 1 Pa at elevated temperature to remove physisorbed material. During this process, irreversible changes of the surface structure (revealed, for example, by a colour change) should be avoided. The highest temperature that can be applied is favourably determined by means of thermogravimetry (see ISO 9277:2010 Figure 3). Otherwise, repeated measurements should be carried out by varying the time and the temperature (see ISO 9277:2010, Figure 4). In addition, the temperatures at which materials are evolved from the sample can be determined by means of differential scanning calorimetry and the gas can be analysed. To obtain reproducible isotherms, it is necessary to carefully control the outgassing conditions. With sensitive samples, a pressure-controlled procedure together with a dedicated heating programme is recommended.

Alternatively to vacuum outgassing, the sample is degassed at an elevated temperature by flushing with a high-quality inert gas, e.g. helium or nitrogen. Complete degassing is indicated by a constant mass or constant pressure, respectively, for a period of 15 min to 30 min. The mass of the dry sample should be determined, recorded to the nearest 0,1 mg.

However, for microporous materials, outgassing under vacuum is recommended as the adsorption measurements often start at relative pressures as low as 10^{-7}. This can be achieved by using a turbomolecular pump which, if coupled with a diaphragm roughing pump, allows the sample to be outgassed even in a completely oil free system.

6.3 Measurement

Adsorption measurements shall be carried out as described in detail in ISO 9277. Here, the importance of the determination of the free space (i.e. the effective void volume) in the manometric method is described, but for micropore measurements which start at very low relative pressures, special caution needs to be applied. The standard procedure uses a non-adsorbing gas such as helium to measure the free space under the operational conditions. However, the use of helium for the free space calibration may be problematic because nanoporous solids with very narrow micropores (e.g. some zeolites, activated carbons) may adsorb non-negligible amounts of helium at cryogenic temperatures (so-called helium entrapment) when - in contrast to helium – the entry of nitrogen or argon molecules is restricted, due to diffusion limitations. If the entrapped helium is not removed prior to the analysis, this can affect significantly the shape of the adsorption isotherm in the ultra-low pressure range. Therefore, if helium is used, the sample should be outgassed after exposure of the sample to helium – at least at room temperature - before continuing the manometric analysis. If possible, it is advantageous to avoid the use of helium for ultramicroporous materials. One way to avoid this problem is to determine the volume of the empty sample cell at ambient temperature using the adsorptive (e.g. nitrogen), followed by the measurement of a calibration curve (with the empty sample cell) performed under the same operational conditions as the adsorption measurements. This calibration curve essentially represents a multipoint free space determination; the necessary correction for the sample volume can be made by means of the skeletal density of the sample.

7 Verification of apparatus performance

A certified reference material selected by the user shall be tested on a regular basis to monitor instrument calibration and performance. In case local reference materials which are offered by a number of national standard bodies are used, they shall be traceable to a certified reference material.

8 Calibration

The calibration of individual components should be carried out according to the manufacturer's recommendations. Typically, calibration of pressure transducers and temperature sensors is accomplished with reference to standard pressure and temperature measuring devices that have calibrations traceable to national standards. Manifold volume calibration is achieved through appropriate pressure and temperature measurements, using constant temperature volumetric spaces or solids of known, traceable volume. Analysis tube calibration is generally accomplished through determination of free space described in ISO 9277.

9 Pore size analysis

9.1 General

The recommended display of adsorption isotherm data depends on whether the focus of the analysis is on assessing microporosity or mesoporosity, For nonporous, macroporous and mesoporous materials the isotherm should be presented in a linear form (see Figure 4), while for microporous samples, favourably, the isotherm $V_a=f(p/p_0)_T$ or $m_a=f(p/p_0)_T$ is represented on a logarithmic scale of the relative pressure (see Figure 5).This allows one to even visually inspect the quality of the experimental data and the effect of micropore structure on the shape of the adsorption isotherm.

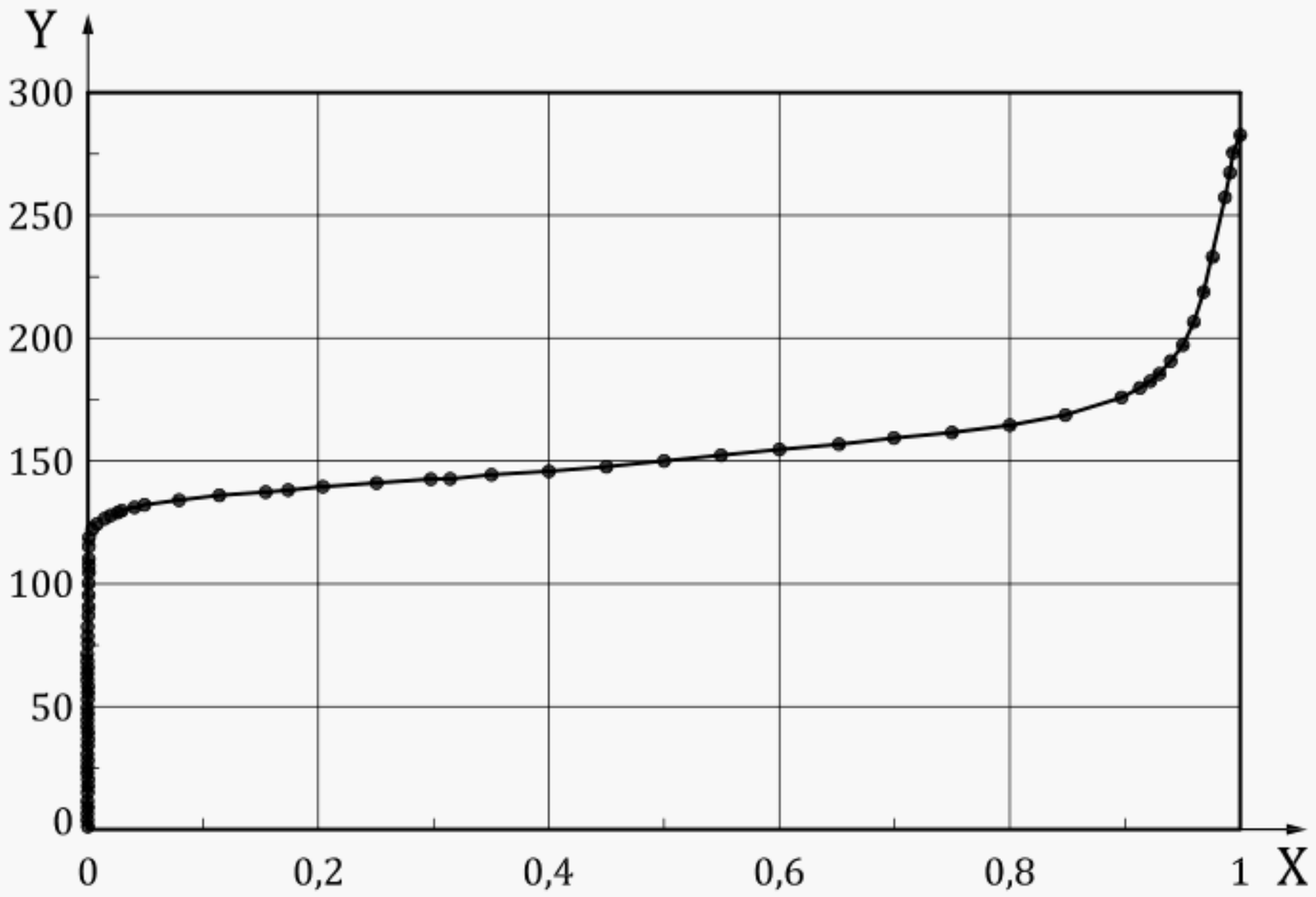

Key

X p/p_0

Y V_g ($cm^3\ g^{-1}$ STP)

Figure 4 — Linear plot of the isotherm (Ar on zeolite at 87,3 K)

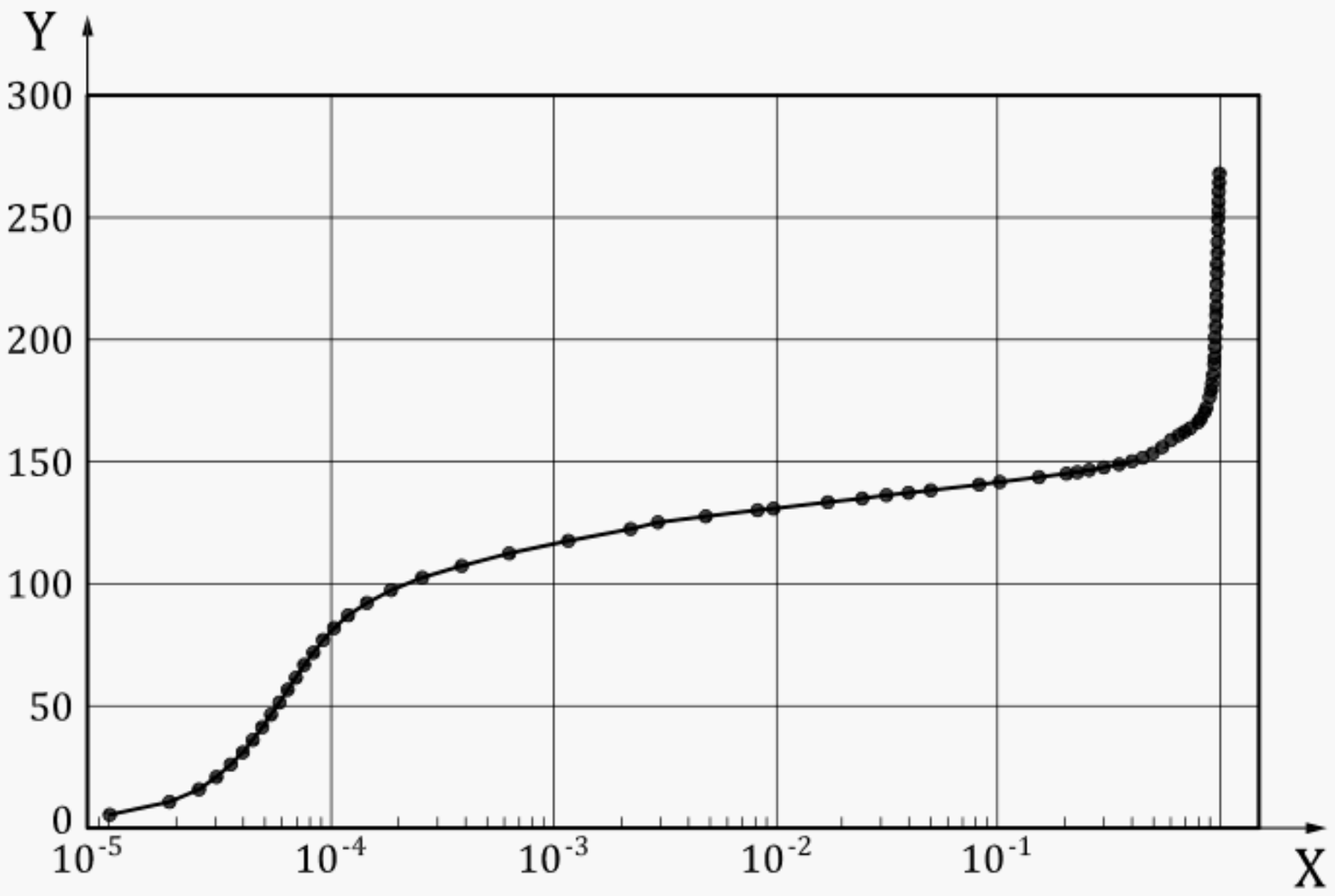

Key

X p/p_0

Y V_g (cm^3 g^{-1} STP)

Figure 5 — Semi-logarithmic plot of the isotherm (Ar on zeolite at 87,3 K)

In order to obtain surface area, pore size distribution, pore volume and other structural information of nanoporous materials from the analysis of gas adsorption isotherms it is necessary to understand the underlying, often quite complex, adsorption mechanisms. This is being addressed in methods available for pore size analysis, which can be divided into so-called classical, macroscopic thermodynamic methods and microscopic methods based on statistical mechanics which describe the adsorbate (e.g. adsorbed layer) on a molecular level.

The state-of-the-art (at the time of publication) for obtaining accurate and reliable pore size distributions over the complete nanopore range is the application of methods based on statistical mechanics and molecular simulation such as methods based on density functional theory (DFT) (e.g. non local density functional theory, NLDFT) and molecular simulation (e.g. grand canonical Monte Carlo simulation, GCMC). Methods for pore size analysis based on DFT and molecular simulation are widely used, commercially available for many important adsorptive/adsorbent systems and recommended by Reference [1]. DFT methods accurately describe adsorption and phase behaviour of fluids confined in pores structures and it has been shown that the application of DFT methods allows one to obtain reliable pore size distributions over the complete range of micro- and mesopores. Classical methods for pore size analysis [e.g. Barrett-Joyner-Halends (BJH), Horvath-Kawazoe (HK), Saito-Foley (SF), Dubinin-Radushkevich (DR)], in addition to not being applicable over the complete nanopore size range, do not realistically treat the state of adsorbed fluid in pore structures and may underestimate the pore size significantly (i.e. by up to 20 % – 30 %, if not properly corrected for pores of width smaller than 10 nm)[1].

9.2 Classical, macroscopic, thermodynamic methods for pore size analysis

9.2.1 Assessment of microporosity

9.2.1.1 Micropore analysis according to Dubinin and Radushkevich

The method originally developed to investigate the microporosity of activated carbons [11]-[14] can be used for any microporous material. By means of Polanyi's potential theory[15] adsorption isotherms of pure gases on microporous sorbents can be described. Each gas/sorbent system is characterized by

an adsorption potential E which is influenced in particular by the chemical properties of the sorbent. The volume V_a filled at a given relative pressure p/p_0 as a part of the total micropore volume V_{micro} is a function of the adsorption potential E:

$$V_a = f(E) \tag{1}$$

According to Dubinin, the adsorption potential equals the work required to bring an adsorbed molecule into the gas phase. For $T < T_{cr}$ using Polanyi's potential yields

$$E = RT \ln \frac{p_0}{p} \tag{2}$$

For the characteristic function Dubinin found the empirical relation

$$V_a = V_{micro} exp\left[-\left\{ \left(\frac{RT}{\beta E_0} \right) \ln \frac{p_0}{p} \right\}^2 \right] \tag{3}$$

The characteristic adsorption energy E_0 characterizes the pore distribution. The affinity coefficient β allows to unite all the curves for each gas at the same adsorbent to one characteristic curve. The Dubinin isotherm now can be written in logarithmic form to give a straight line:

$$\lg V_a = \lg V_{micro} - D \left[\lg \frac{p_0}{p} \right]^2 \tag{4}$$

with

$$D = 2{,}303 \left(\frac{RT}{\beta E_0} \right)^2 \tag{5}$$

The evaluation data of the region of relative pressure $10^{-4} < p/p_0 < 0{,}1$ should be preferred. The data are registered in a diagram $\lg V_a$ versus $\left[\lg \frac{p_0}{p} \right]^2$ (see Figure 6). The slope of the regression line gives the parameter D. From the ordinate intercept, the total micropore volume V_{micro} can be calculated.

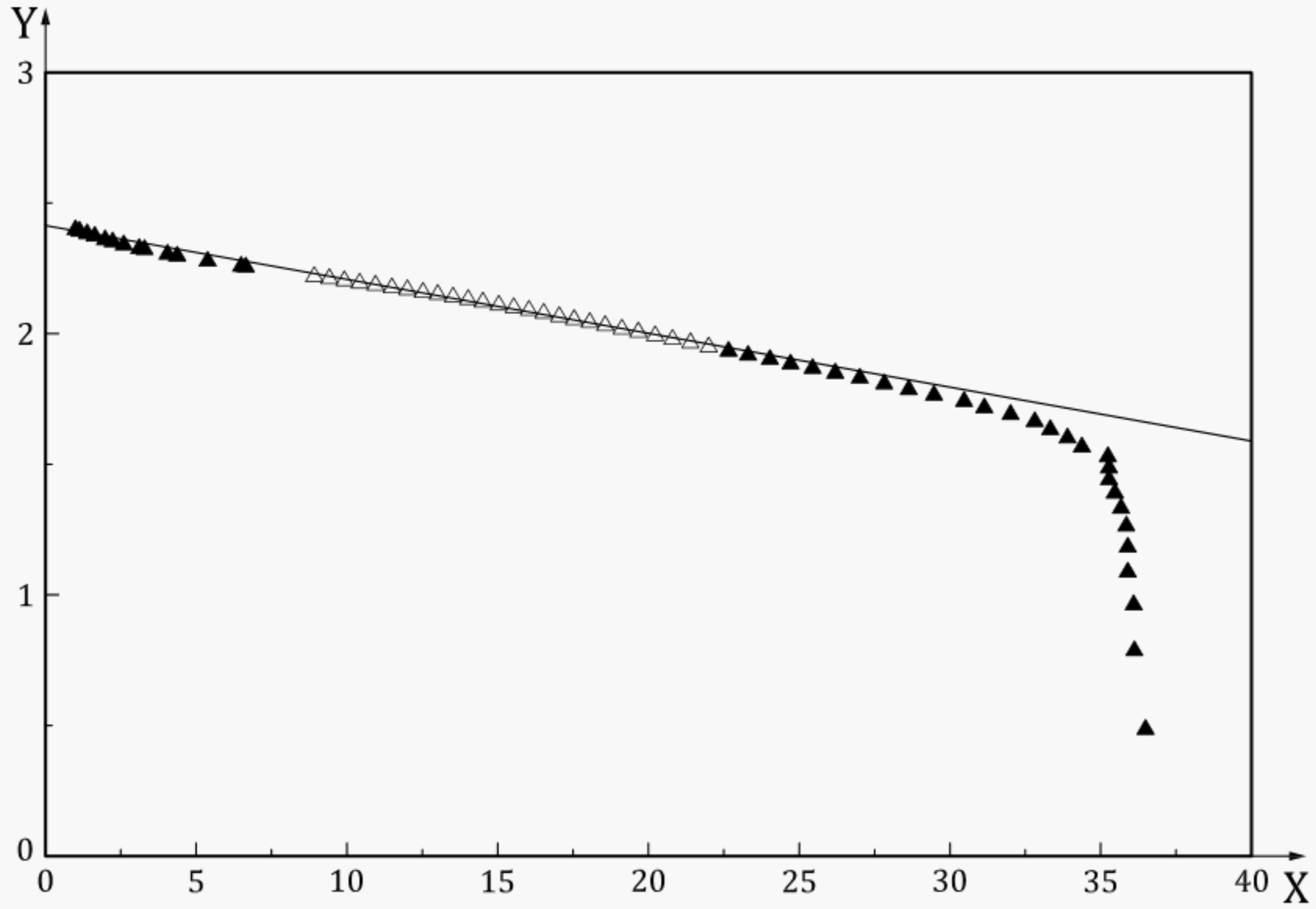

Key

X	$[\log_{10}(p/p_0)]^2$
Y	$\log_{10}(V_a/(\mathrm{cm}^3\ \mathrm{g}^{-1}))$
▲	experimental data points
△	experimental data points used for DR fit
———	DR fit line

Figure 6 — Dubinin-Radushkevitch (DR) plot of an adsorption isotherm of N_2 at 77 K on activated carbon

9.2.1.2 Micropore analysis by comparison of isotherms

In this method of analysis, gas adsorption isotherms on a sample are compared with that on a non-porous reference material of similar chemical surface composition. The procedure is depicted in Figure 7.

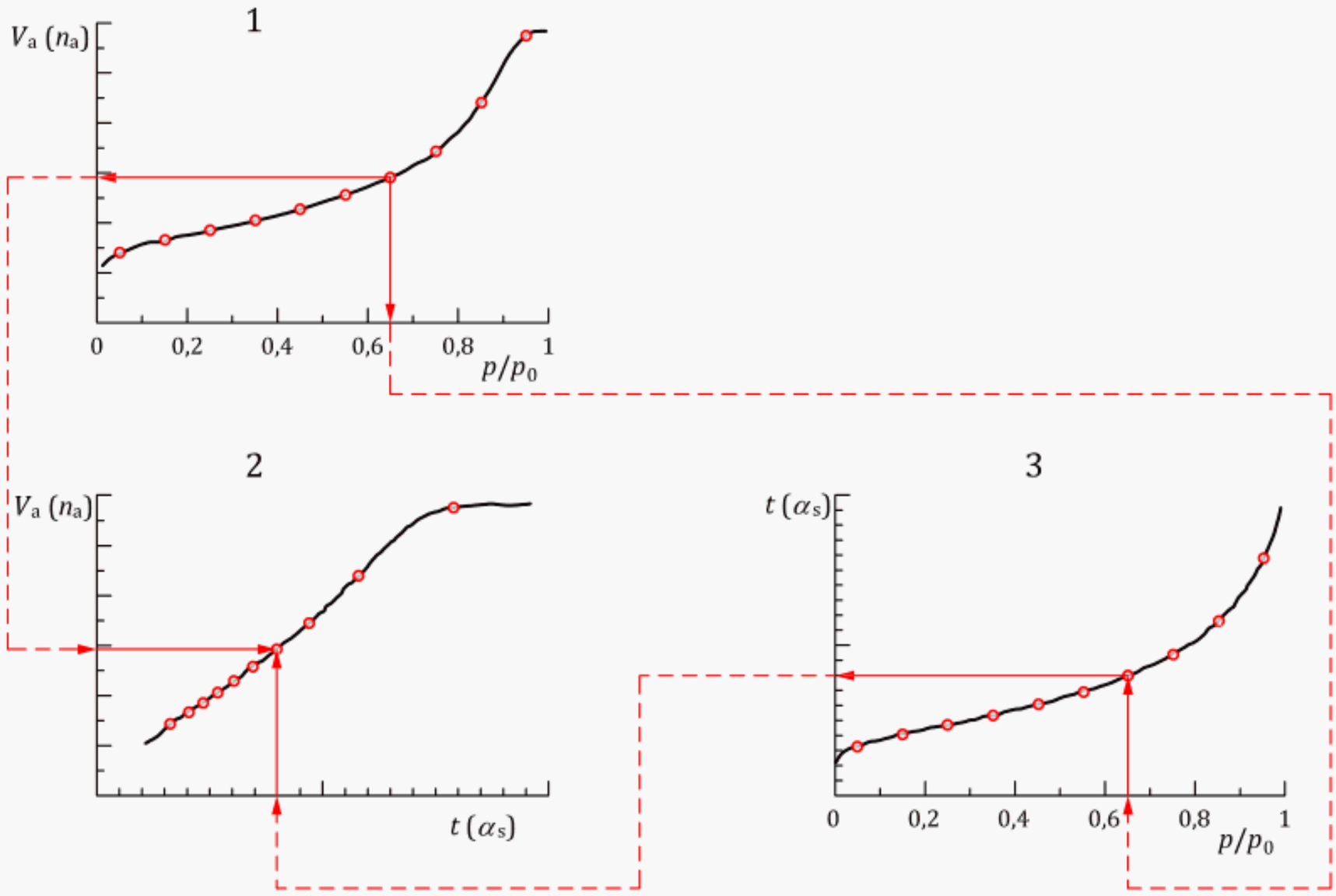

Key

1 sample isotherm
2 resulting comparison diagram
3 reference isotherm

Figure 7 — Schematic representation of the design of a comparison diagram

In a comparison plot diagram, the sorption isotherm under test is redrawn as a *t*-plot or α_s plot, i.e. the change of the adsorbed amount is plotted against t or α_s values instead of p/p_0. Characteristic comparison plots are depicted in Figure 8.

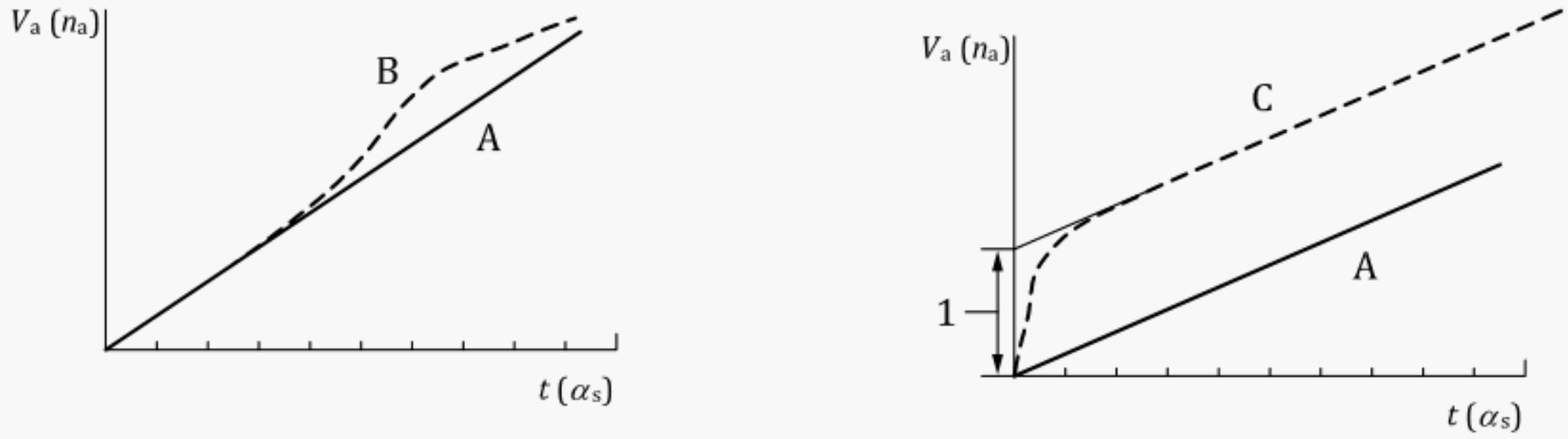

Key

1 extrapolated ordinate intercept for V_{micro}

Figure 8 — Isotherms (top) and comparison diagrams (bottom) of nonporous (A), mesoporous (B) and microporous materials (C)

Preconditions for a consistent interpretation of a comparison diagram are:

— a smooth sample surface in the mesopore region;

— micropore filling and capillary condensation occur well separated one after the other.

Multilayer adsorption results in a straight line in the comparison diagram. However, pores cause an upwards deviation which allows for an assessment of the pore volume which can be assigned to a certain region of pore width. Within linear parts, the specific surface area a_s of the not yet filled pores may be calculated from the slope b:

$$a_s = b\frac{a_{s,ref}}{b_{ref}} \tag{6}$$

where $a_{s,ref}$ and b_{ref} refer to the specific surface area and the slope of the reference material. The ordinate intercept corresponds to the volume of pores filled in the respective region at this relative pressure.

A high portion of micropores causes a steep increase in the initial part of the curve followed by a linear part. For exclusively microporous materials the slope of the linear part corresponds to the external surface and otherwise to the external plus the surface of the mesopore/macropore walls. The extrapolated ordinate intercept of the linear part gives the micropore volume V_{micro} to be calculated by means of $V_a = m_a/(\rho_l \cdot m_s)$. If there are no micropores, the initial part is linear, and the specific surface area equals that calculated by the method of Brunauer, Emmett and Teller (see ISO 9277).

9.2.1.3 *t*-plot method

With the *t*-plot method according to Lippens and deBoer [16]-[18] the adsorbed amount is depicted as a function of the statistical layer thickness t, calculated from a standard isotherm of a non-porous sample:

$$t = \frac{V_a}{a_s} = \frac{n_a}{n_m}\sigma_t \tag{7}$$

where σ_t represents the thickness of single molecular layer, usually taken as 0,354 nm for nitrogen. The specific surface area a_s or the monolayer capacity n_m of the reference sample may be determined according to ISO 9277. Formula (7) can be applied for any combination of inert gas/adsorbent. It allows for the choice of a reference material with surface of similar chemical composition. With nitrogen at

77 K and using a molecular cross-sectional area a_m = 0,162 nm^2 and assuming a tight hexagonal packing of the liquid adsorbate with density 0,807 9 g cm^{-3} Formula (8) becomes

$$t = 0{,}354 \frac{V_a}{V_m} = 0{,}354 \frac{n_a}{n_m} \tag{8}$$

In this case the layer thickness t (which represents an average thickness) may be taken from a universal t-curve as published in the literature (see Bibliography).

From the slope of the line depicted in the t diagram the specific surface area may be calculated using Formula (8) If the adsorbed volume is given in cm^3 g^{-1} at STP state and the layer thickness t in nm, the slope dV_a/dt has the dimension cm^3 g^{-1} nm^{-1}, then the specific surface area results in m^2 g^{-1} when applying Formula (9):

$$a_s = 1{,}546\,8 \frac{\Delta V_a}{\Delta t} \tag{9}$$

The micropore volume V_{micro} results from the ordinate intercept then as

$$V_{micro} = 0{,}001\,546\,8\, V_a \tag{10}$$

In Formula (10), it is assumed that the density of nitrogen in the micropores is equal to the density of liquid nitrogen. The factor 0,001 546 8 converts the nitrogen volume at STP state into the corresponding liquid volume. V_{micro} should be considered as an 'effective' micropore volume, which acknowledges that this is an oversimplification, as the density of nitrogen in micropores may not be equal to the liquid density.

9.2.1.4 α_s-method

This method abstains from the calculation of the layer thickness. Instead the adsorption at the reference sample is related to a selected relative pressure[19]. In general p/p_0 = 0,4 is used because at this relative pressure (for nitrogen at 77 K) the monolayer is complete but capillary condensation has not yet started for most materials (with exception of adsorbents which possess mesopores with pore diameters in the range between 2 nm and 5 nm. The reference value α_s is calculated using the reference isotherm as follows:

$$\alpha_s = \frac{V_a}{V_a(0{,}4)} = \frac{n_a}{n_a(0{,}4)} \tag{11}$$

In the α_s diagram the measured adsorbed amount is depicted as a function of α_s. The α_s diagram looks like the t diagram and may be evaluated for the calculation of the specific surface area and the micropore volume in the same manner.

9.2.1.5 Determination of micropore size distribution by the Horvath-Kawazoe (HK) and Saito-Foley (SF) method

Horvath and Kawazoe (HK)[20],[21] described a semi-empirical, analytical method for the calculation of effective pore size distributions from nitrogen adsorption isotherms in microporous materials. The original HK approach is based on the work of Everett and Powl[23] and considers a fluid (nitrogen) confined to a slit-pore, such as they can be found in some carbon molecular sieves and active carbons. Everett and Powl calculated the potential energy profiles for noble gas atoms adsorbed in a slit between two graphitized carbon layer planes. The separation between nuclei of the two layers is l. The adsorbed fluid is considered as a bulk fluid influenced by a mean potential field, which is characteristic of the adsorbent-adsorbate interactions. The term "mean field" indicates that the potential interactions between an adsorbate molecule and the adsorbent, which may exhibit a strong spatial dependence, are replaced by an average, uniform potential field. Horvath and Kawazoe found by using thermodynamic arguments that this average potential can be related to the free energy change of adsorption yielding a

relation between filling pressure and the effective pore width $d_p = l - d_s$, where d_s is the diameter of an adsorbent molecule:

$$\ln\left(\frac{p}{p_0}\right)=\frac{N_A}{RT}\frac{(N_s A_s + N_a A_a)}{\sigma^4 (l-2d_0)} f_{HK}(\sigma,l,d_0) \tag{12}$$

with

$$f_{HK}(\sigma,l,d_0)=\frac{\sigma^4}{3(l-d_0)^3}-\frac{\sigma^{10}}{9(l-d_0)^9}-\frac{\sigma^4}{3(d_0)^3}+\frac{\sigma^{10}}{9(d_0)^9}$$

The parameters d_0, σ, A_s and A_a can be calculated using the following formulae:

$$d_0=\frac{d_a+d_s}{2} \tag{13}$$

$$\sigma=\left(\frac{2}{5}\right)^{\frac{1}{6}} d_0 \tag{14}$$

$$A_s=\frac{6 m_e c^2 \alpha_{s*} \alpha_a}{\frac{\alpha_{s*}}{\chi_s}+\frac{\alpha_a}{\chi_a}} \tag{15}$$

$$A_a=\frac{3}{2} m_e c^2 \alpha_a \chi_a \tag{16}$$

According to Formula (12) the filling of micropores of a given size and shape takes place at a characteristic relative pressure. This characteristic pressure is directly related to the adsorbent-adsorbate interaction energy.

Saito and Foley [23],[24] extended the HK method for the calculation of effective pore size distributions of zeolites from argon adsorption isotherms at 87 K. The Saito and Foley (SF) method is based as HK on the Everett and Powl potential equation, but now for a cylindrical pore geometry. Following the logic of the HK derivation, Saito and Foley derived an equation similar to the HK equation which relates the micropore filling pressure to the (effective) pore diameter $d_p = l - d_s$:

$$\ln\left(\frac{p}{p_0}\right)=\frac{3}{4}\frac{\pi N_A}{RT}\frac{(N_s A_s + N_a A_a)}{{d0}^4} f_{SF}(\alpha,\beta,l,d_0) \tag{17}$$

with

$$f_{SF}(\alpha,\beta,l,d_0)=\sum_{k=0}^{\infty}\left[\frac{1}{1+k}\left(1-\frac{2d_0}{l}\right)^{2k}\left\{\frac{21}{32}\alpha_k\left(\frac{2d_0}{l}\right)^{10}-\beta_k\left(\frac{2d_0}{l}\right)^4\right\}\right]$$

The parameter A_s and A_a can be calculated according to Formulae (16) and (17). Parameters α_k and β_k are defined as:

$$\alpha_k=\left(\frac{-4{,}5-k}{k}\right)^2 \alpha_{k-1} \tag{18}$$

$$\beta_k=\left(\frac{-1{,}5-k}{k}\right)^2 \beta_{k-1} \tag{19}$$

with $\alpha_0 = \beta_0 = 1$

In order to perform the HK and SF calculations the values for the adsorbent parameters α_s, χ_s, d_s, N_s as well as of the adsorptive parameters α_a, χ_a, d_a and N_a need to be known. The results are very sensitive with regard to the choice of these constants. Annex A gives material parameters for the systems nitrogen/carbon and argon/zeolite.

9.2.2 Assessment of meso/macroporosity

9.2.2.1 Pore volume

If a mesoporous adsorbent contains no macropores, its Type IV isotherm remains nearly horizontal over the upper range of p/p_0. The pore volume, V_p, is then derived from the amount of vapour adsorbed at a relative pressure close to unity (e.g. p/p_0 = 0,95), by assuming that the pores are filled with the adsorbate in the bulk liquid state. If macropores are present, the isotherm is no longer nearly horizontal near p/p_0 = 1 and the total pore volume cannot be evaluated from such a composite Type IV and Type II isotherm.

9.2.2.2 Assessment of meso/macropore size distribution by Kelvin equation based approaches

The many methods for mesopore size analysis, which make use of the modified Kelvin equation, include those proposed by Barrett, Joyner and Halenda (BJH) and Broeckhoff and de Boer[2],[4]. In order to account for the preadsorbed multilayer film, the Kelvin equation is combined with a standard isotherm (the *t*-curve), which is determined on certain well-defined nonporous solids.

For cylindrical pores the modified Kelvin equation is:

$$\ln(p/p_0) = -2\gamma V_m/\mathrm{RT}(r_p - t_c) \quad (20)$$

where

γ is the surface tension;

T is the temperature;

V_m is the molar volume of the condensed liquid;

R is the gas constant;

r_p is the pore radius;

t_c is the thickness of the adsorbed multilayer film, which is formed prior to pore condensation.

However, for the size analysis of narrow mesopores, the standard t-curve is not entirely satisfactory, because the curvature and enhanced surface forces are not properly taken into account. Similarly, the validity of the Kelvin equation is questionable as the mesopore width is reduced because macroscopic concepts can no longer be safely applied. This was clearly demonstrated with the aid of model mesoporous molecular sieves (e.g. M41S materials). Because of their high degree of order, the pore diameter of such model substances can be derived by independent methods (X-ray-diffraction, high-resolution transmission electron microscopy, etc.). It was shown that the Kelvin equation based procedures, such as the BJH method, significantly underestimate the pore size for narrow mesopores (for pore diameter < ~ 10 nm the pore size will be underestimated by ~ 20 % – 30 %).The limitations of the Kelvin equation can be avoided by applying microscopic methods based on molecular simulation or DFT (e.g. NLDFT) which as yield the thermodynamics and density profiles of confined fluids and a description of the adsorbed phase on a molecular level. They capture the essential features of both micropore and mesopore filling and hysteresis. As a consequence, they allow one to obtain a more reliable assessment of the pore size distribution over the complete range Furthermore, one can obtain useful information from both the adsorption and desorption branches of the hysteresis loop. With certain ordered mesoporous materials, these methods are capable of quantitatively predicting the pore condensation and hysteresis behaviour by taking into account the underlying adsorption-desorption

mechanisms including the delay in condensation due to metastability of the pore fluid. These advantages are crucial in the pore size analysis of materials which give rise to H2, H3, H4 and H5 hysteresis loops.

9.3 Advanced, microscopic approaches based on density functional theory and molecular simulation

9.3.1 General

Methods based on density functional theory (e.g. non local density functional theory (NLDFT)) and computer simulation methods (e.g. grand canonical Monte Carlo simulation, GCMC))[25]-[42] have been developed into powerful methods for the description of sorption and phase behaviour of inhomogeneous fluids, confined to porous materials These methods allow one to calculate equilibrium density profiles of a fluid adsorbed on surfaces and in pores from which the adsorption isotherms, heats of adsorption and other thermodynamic quantities can be derived. Compared to the classical thermodynamic, macroscopic models the NLDFT and GCMC based methods describe the behaviour of fluids confined in the pores on a molecular level. This allows one to relate molecular properties of gases with their adsorption properties in pores of different sizes. It follows that pore size characterization methods based on the NLDFT approach are applicable to the whole range of micropores and mesopores.

Commercial DFT and GCMC software is now available for various adsorbent systems and pore geometries (cylindrical, slit, spherical or hybrids). However, as already discussed, it is important to ensure that the chosen DFT and molecular simulation based methods are compatible with the experimental nanoporous system.

9.3.2 Application for pore size analysis: Kernel and integral adsorption equation

To practically apply the theory for the calculation of the pore size distributions from the experimental adsorption isotherms, theoretical model isotherms needs to be calculated using methods of statistical mechanics. These isotherms are calculated by integrating of the equilibrium density profiles, $\rho(\boldsymbol{r})$, of the fluid in the model pores. A set of isotherms calculated for a set of pore sizes in a given range for a given adsorbate constitutes the model database. Such a set of isotherms called a kernel can be regarded as a theoretical reference for a given adsorption system and as such can be used to calculate pore size distributions from adsorption isotherms measured for the corresponding systems.

It is important to realize that the numerical values of a given kernel depend on a number of factors such as the assumed geometrical pore model, values of the gas-gas and gas-solid interaction parameters, and other model assumptions. It is a general practice to adjust interaction parameters (fluid-fluid and fluid-solid) in such a way that the model would correctly reproduce fluid bulk properties (e.g. bulk liquid-gas equilibrium densities and pressures, liquid-gas interfacial tensions). Correct prediction of the surface tension is a necessary condition for any model used for the quantitative description of the capillary condensation/desorption transition in pores. The parameters of the solid-fluid potential are chosen to fit the standard adsorption isotherms on well-defined non-porous adsorbents[27].

A number of adsorption models were studied and parameters evaluated for gas adsorption on various materials are published in the literature. For instance, gas-gas- and gas-solid interaction parameters for the systems nitrogen/carbon, carbon dioxide/carbon and argon/carbon can be found in References [26],[27],[28],[36],[37]. Appropriate interaction parameters for the systems nitrogen/silica and argon/silica are given in References [28],[37]. References to the values of parameters used for the DFT analysis of several adsorption systems are listed in Tables B.1 and B.2.

The calculation of pore size distribution is based on a solution of the integral adsorption equation (IAE) [4], which correlates the kernel of theoretical adsorption/desorption isotherms with the experimental sorption isotherm. The IAE equation is given as:

$$N(p/p_0) = \int_{W_{\mathrm{MIN}}}^{W_{\mathrm{MAX}}} N(p/p_0, W) f(W) \mathrm{d}W \tag{21}$$

where

$N(p/p_0)$ is the adsorbed volume data (from the experimental sorption isotherm);

W is the pore width (distance between opposite walls of slit; diameter of cylindrical and spherical pores);

$N(p/p_0,W)$ is the kernel of the theoretical isotherms in pores of different widths;

$f(W)$ is the pore size distribution function.

The IAE equation reflects the assumption that the total isotherm consists of a number of individual "single pore" isotherms multiplied by their relative distribution, $f(W)$, over a range of pore sizes. The set of $N(p/p_0,W)$ isotherms (kernel) for a given system (adsorptive/adsorbent) can be obtained by either density functional theory or molecular simulation (e.g. Monte Carlo computer simulation). The pore size distribution is then derived by solving the IAE equation numerically. In general, the solution of the IAE represents an ill-posed problem, which requires some degree of regularization. The existing regularization algorithms[40],[41] allow to obtain meaningful and stable solutions of this equation. In order to confirm the validity of the calculation, the calculated NLDFT (or GCMC) (fitting) isotherm shall be compared with the experimental sorption isotherm.

10 Reporting

A summary of the measurement conditions and constants used in the calculation should be provided with each result as follows.

a) Laboratory, operator, date.

b) Sample identification, e.g. chemical composition, purity, particle size distribution, method of sampling, sample division.

c) Sample source.

d) Mass of outgassed sample m_s in g.

e) Experimental method and instrument used.

f) Sample pre-treatment.

g) Outgassing conditions: temperature and evacuation pressure.

h) Calibration constants.

i) Used model/method for pore size and surface area analysis.

j) Materials parameter for adsorptive and adsorbent in case of SF and HK method is applied.

k) Description of kernel (e.g. adsorptive/adsorbent pair, assumed pore geometry, adsorption/desorption branch) in case NLDFT method is applied.

l) Micropore volume [$cm^3 \cdot g^{-1}$].

m) Total pore volume [$cm^3 \cdot g^{-1}$].

n) Plots and tables of cumulative pore volume, and pore volume distribution (for HK, SF, and NLDFT method).

Annex A
(informative)

Horvath-Kawazoe and Saito-Foley method

A.1 Examples for material constants, adsorbent and adsorptive parameters

Examples for adsorptive and adsorbent model parameters for application in Horvath-Kawazoe and Saito-Foley methods are given in Tables A.1 and A.2. The constants were taken from the original papers of Horvath, Kawazoe and Saito-Foley. Nonuniform values of the parameters given in the Tables A.1 and A.2 can be found in the literature. Hence, in order to present significant results, it is crucial that the adsorbent and adsorptive parameter employed in the SF and HK calculations are always stated in the analysis report.

Table A.1 — Adsorbent parameters

Physical quantity	**Symbol**	Carbon References [19] and [20]	Zeolite References [21] and [22]
Polarizability [10^{-24} cm^3]	α_{s*}	1,02	2,50
Magnetic susceptibility [10^{-29} cm^3]	χ_s	13,5	1,30
Surface density (atoms per m^2 of pore wall) [10^{19} m^{-2}]	N_s	3,84	1,31
Diameter [nm]	d_s	0,34	0,28

Table A.2 — Adsorptive parameters

Physical quantity	**Symbol**	Nitrogen References [19] and [20]	Argon References [21] and [22]
Polarizability [10^{-24} cm^3]	α_a	1,46	1,63
Magnetic susceptibility [10^{-29} cm^3]	χ_a	2,00	3,25
Surface density (atoms per m^2 of monolayer) [10^{18} m^{-2}]	N_a	6,70	8,52
Diameter [nm]	d_s	0,30	0,34

Table A.3 — Relation between the pore diameter and the relative pressure where micropore filling of nitrogen occurs at 77,35 K in a carbon slit pore according to Horvath-Kawazoe

d_p [nm]	0,4	0,5	0,6	0,7	0,8	1,0	1,2	1,4	1,7	2,0
p/p_0	$1{,}8 \times 10^{-7}$	$1{,}2 \times 10^{-5}$	$1{,}7 \times 10^{-4}$	$9{,}6 \times 10^{-4}$	$3{,}2 \times 10^{-3}$	$1{,}4 \times 10^{-2}$	$3{,}5 \times 10^{-2}$	$6{,}3 \times 10^{-2}$	$1{,}1 \times 10^{-1}$	$1{,}6 \times 10^{-1}$

The calculation in Table A.3 was performed by using the materials constants for adsorptive and adsorbents given in Tables A.1 and A.2

Table A.4 — Relation between the pore diameter and the relative pressure where micropore filling of argon occurs at 87,27 K in a cylindrical zeolite pore according to the Saito-Foley approach

d_p [nm]	0,4	0,5	0,6	0,7	0,8	1,0	1,2	1,4	1,7	2,0
p/p_0	$5{,}7 \times 10^{-7}$	$9{,}8 \times 10^{-6}$	$1{,}4 \times 10^{-4}$	$8{,}7 \times 10^{-4}$	$3{,}1 \times 10^{-3}$	$1{,}5 \times 10^{-2}$	$3{,}9 \times 10^{-2}$	$7{,}2 \times 10^{-2}$	$1{,}3 \times 10^{-1}$	$1{,}9 \times 10^{-1}$

The calculation in Table A.4 was performed by using the materials constants given in Tables A.1 and A.2.

A.2 Application example for Saito-Foley micropore analysis

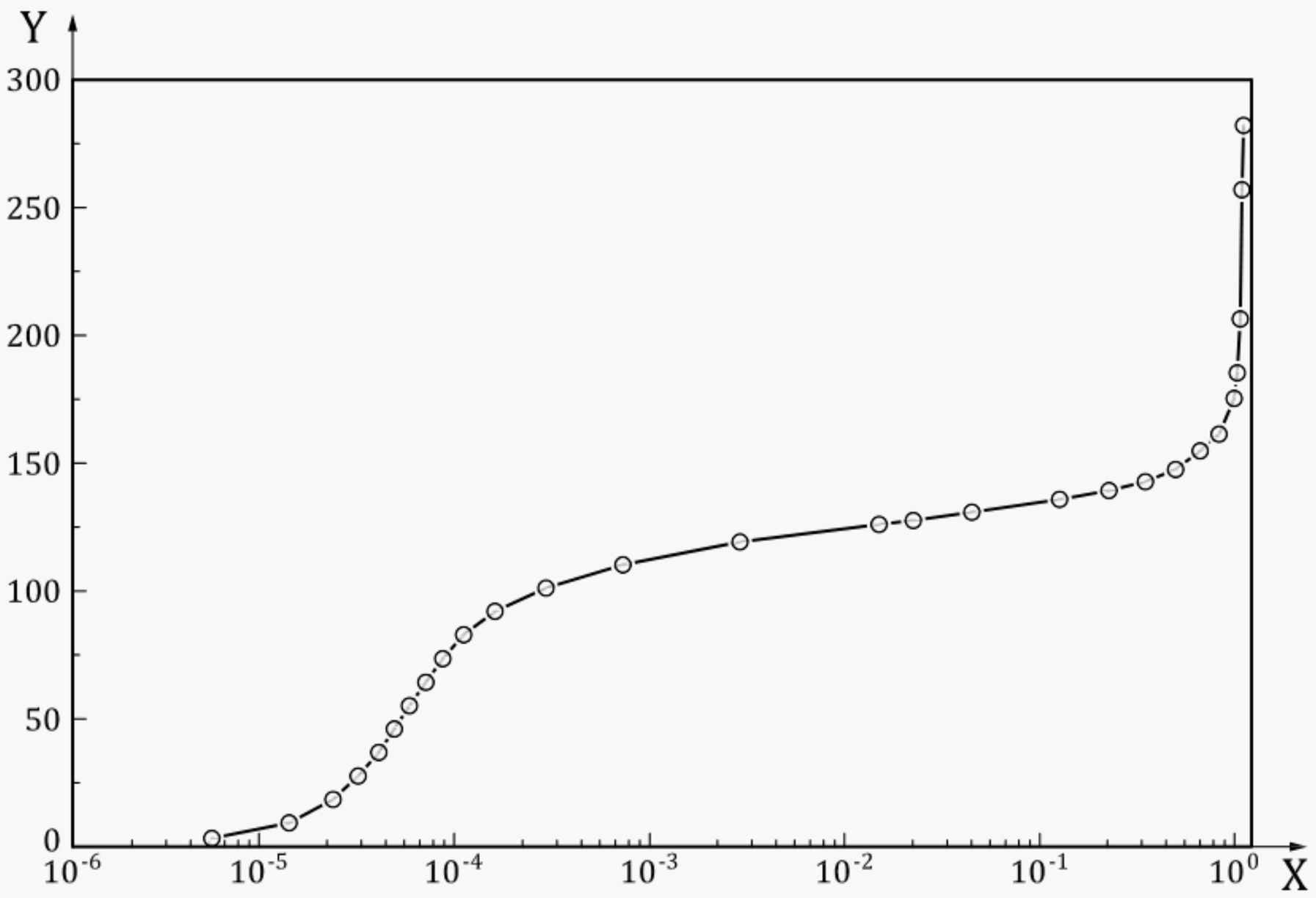

Key

X p/p_0

Y V_g ($cm^3\ g^{-1}$ STP)

Figure A.1 — Experimental argon (87,3 K) adsorption isotherm on a type A zeolite

Figure A.2 is obtained from the argon sorption isotherm shown in Figure A.1.

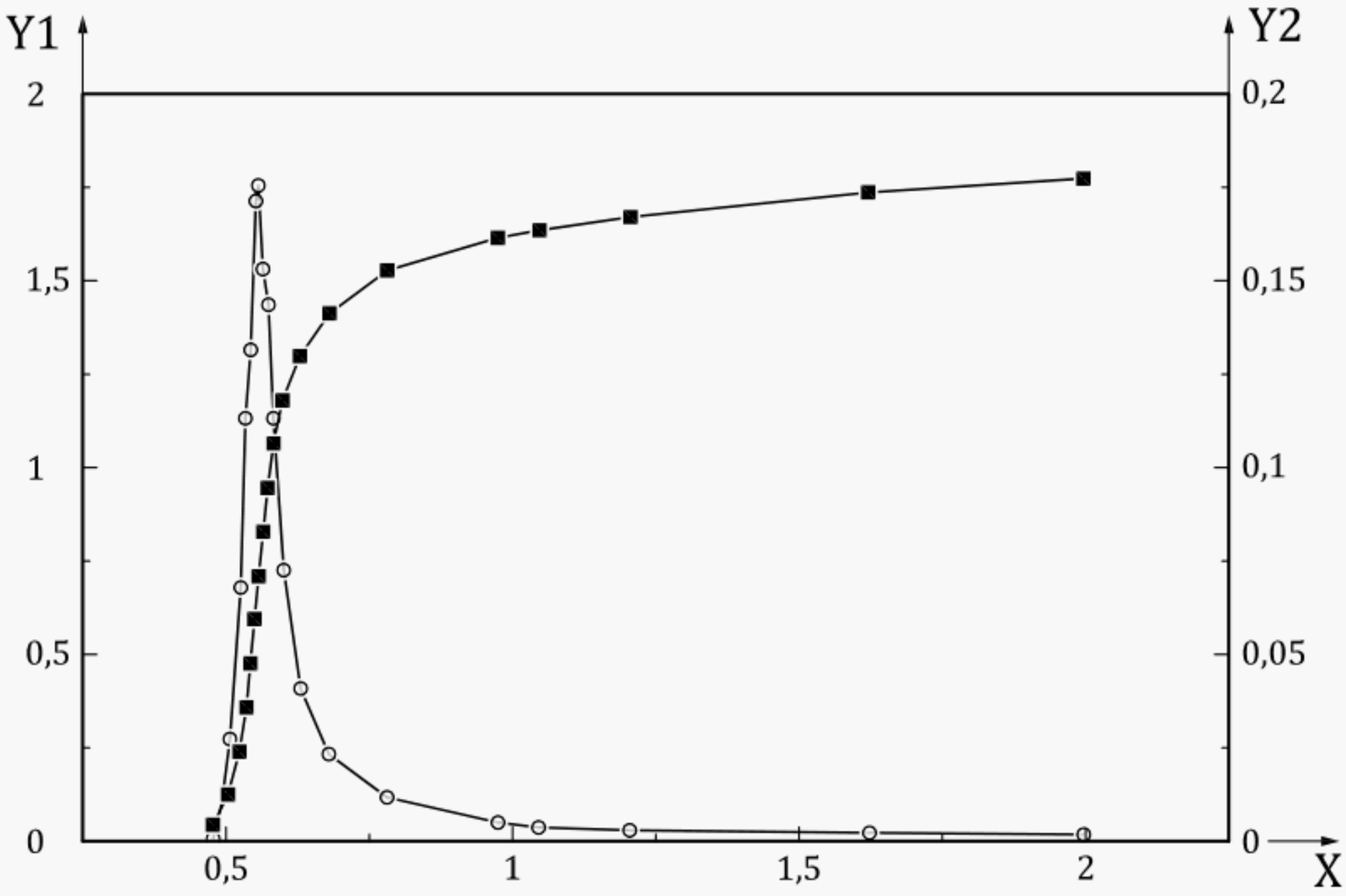

Key

X	pore diameter (nm)
Y1	differential pore volume ($cm^3g^{-1}nm^{-1}$)
Y2	cumulative micropore volume (cm^3g^{-1})
—■—	cumulative micropore volume
—○—	differential micropore volume

NOTE The adsorptive and adsorbent parameters used in the calculation correspond to the values given in Tables A.1 and A.2

Figure A.2 — Saito-Foley pore size analysis of type A zeolite

Annex B
(informative)

NLDFT method

B.1 Examples of adsorptive and adsorptive-adsorbent interaction parameters for use in NLDFT calculations

Table B.1 — Parameters of the adsorptive-adsorptive intermolecular potentials for NLDFT calculations

Gas	ε_{ff}/k_B K	σ_{ff} nm	δHS nm
Nitrogen [a]	94,45	0,357 5	0,357 5
Argon [b]	118,05	0,330 5	0,338 0
Carbon dioxide [a]	235,9	0,345 4	0,349 5

[a] See References [29] and [37].

[b] See Reference [37].

Table B.2 — Parameters for adsorptive-adsorbent intermolecular potentials for NLDFT calculations

Gas-solid	ε_{sf}/k_B K	σ_{sf} nm	N_s
Nitrogen-carbon [b]	53,22	0,349 4	Carbon [a]: N_s = 38,19 nm^{-2}
Carbon dioxide-carbon [b]	81,5	0,343 0	—
Nitrogen-silica [c]	147,3	0,317 0	Silica [a]: N_s = 15,3 nm^{-2}
Argon-silica [d]	171,24	0,300 0	—

[a] See References [28], [29], [37].

[b] See References [29], [37].

[c] See References [28], [37].

[d] See References [29], [37].

B.2 Example of the application of NLDFT micropore analysis

The plot in Figure B.1 was obtained by assuming a slit-pore model and using the adsorptive/adsorbent parameters as given in Tables B.1 and B.2 [28],[37].

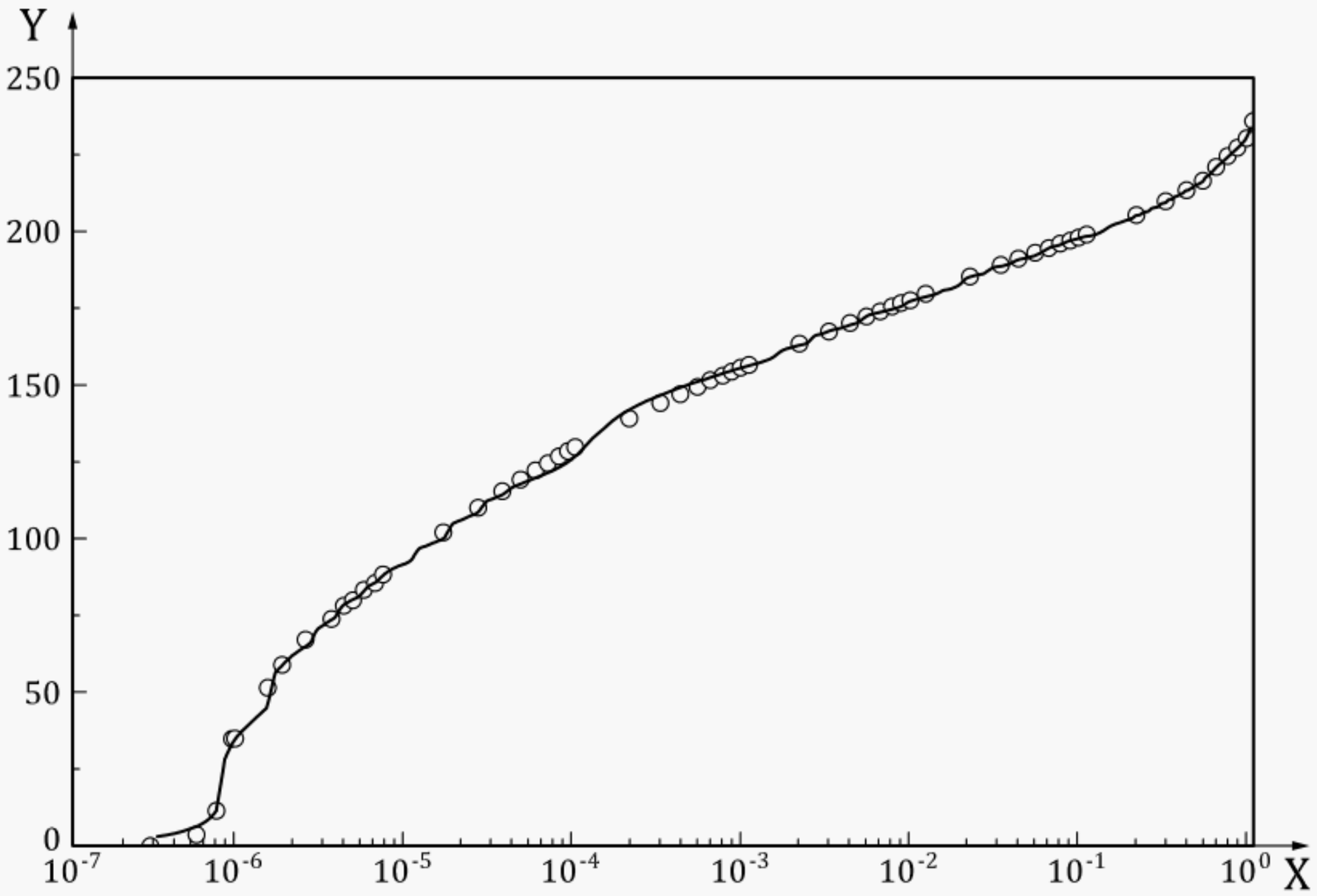

Key

X p/p_0

Y V_g ($cm^3\ g^{-1}$ STP)

NOTE Obtained by assuming a slit pore model and adsorptive/adsorbent parameters as given in Tables B.1 and B.2 from Reference [36]).

Figure B.1 — Experimental nitrogen (at 77,3 K) adsorption isotherm on an activated carbon fibre (ACF) and NLDFT-fit

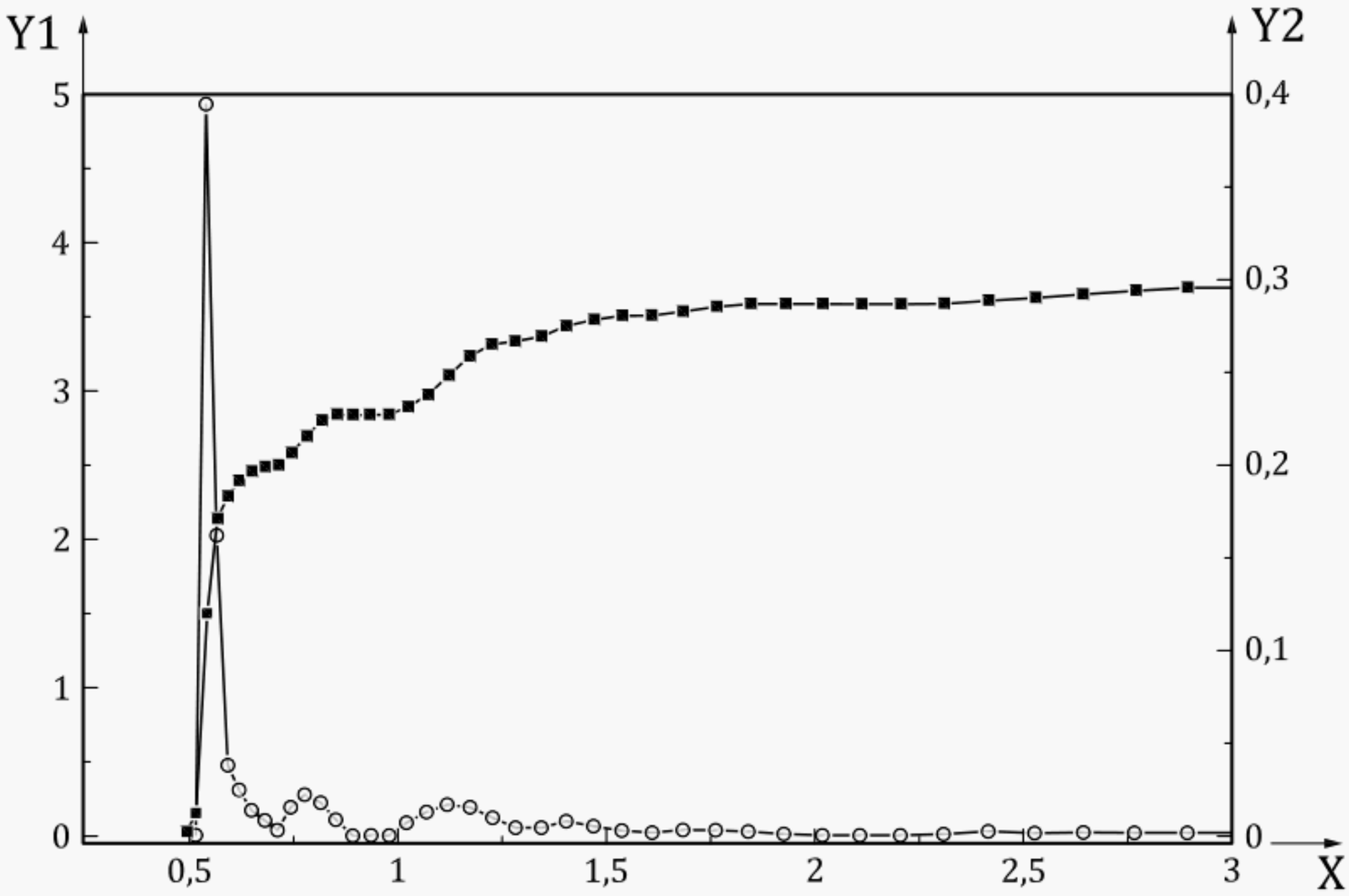

Key

X	pore diameter (nm)
Y1	differential pore volume ($cm^3g^{-1}nm^{-1}$)
Y2	cumulative micropore volume (cm^3g^{-1})
—■—	cumulative micropore volume
—○—	differential micropore volume

NOTE The calculations were performed based on a slit-pore model. The adsorptive and adsorbent interaction parameters used in the calculations are given in Tables B.1 and B.2 (from Reference [33]).

Figure B.2 — NLDFT pore size analysis of activated carbon fibre obtained from the nitrogen adsorption isotherm shown in Figure B.1

Bibliography

[1] Thommes M., Kaneko K., Neimark A.V., Olivier J.P. F., Rodriguez-Reinoso J., Rouquerol, K.S.W. Sing. Pure Appl. Chem. 2015, **87** p. 1051

[2] Gregg S.J., Sing K.S.W., Adsorption, Surface Area and Porosity. Academic Press, London, Second Edition, 1982

[3] Mikhail R., Sh., Robens E. *Microstructure and Thermal Analysis of Solid Surfaces.* Wiley, Chichester, 1983

[4] Kaneko K., J. Membr. Sci. 1994, **96** p. 59

[5] Ross S., Olivier J.P., On Physical Adsorption. Wiley and Sons, New York, 1964[

6] Conner W.C., In: Physical Adsorption: Experiment, Theory and Applications. (Fraissard J., ed.). Kluwer, Dordrecht, 1997, pp. 33–63

[7] Lowell S., Shields J.E., Thomas M.A., Thommes M., Characterization of Porous Solids and Powders: Surface Area, Pore Size and Dennity. Kluwer, Dordrecht, 2004

[8] Rouquerol J., Rouquerol F., Sing K.S.W. P., Llewellyn, G. Maurin, Adsorption by Powders and Porous Solids: Principles, Methodology and Applications, Academic Press, 2014

[9] Cychosz K.A., Guillet-Nicolas R., Garcia-Martinez J., Thommes M., Chem. Soc. Rev. 2017, **46** p. 389

[10] Dubinin M.M., Q. Rev. Chem. Soc. 1955, **9** p. 101

[11] Dubinin M.M., Chem. Rev. 1969, **60** p. 235

[12] Stoeckli H.F. *J. Colloid Interface Sci.* **59** (1977) 1, 185

[13] Dubinin M.M., Stoeckli H.F., J. Colloid Interface Sci. 1980, **75** p. 34

[14] Polanyi M., Verh. dtsch. physik. Ges. 1914, **16** p. 1012

[15] Lippens B.C., Linsen B.G., deBoer J.H., J. Catal. 1964, **3** p. 32

[16] Lippens B.C., deBoer J.H., J. Catal. 1965, **4** p. 319

[17] deBoer J.H., Linsen B.G., Osinga Th.J. J. Catal. 1965, **4** p. 643

[18] Sing K.S.W., In: Surface Area Determination. (Everett D.H., Ottewill R.H., eds.). Butterworths, London, 1970, pp. 25

[19] Horvath G., Kawazoe K., J. Chem. Eng. of Jpn. 1983, **16** p. 470

[20] Horvath G., Energetic interactions in phase and molecular level pore characterization in nano-range. Colloids Surf. A Physicochem. Eng. Asp. 1998, **141** pp. 295–304

[21] Everett D.H., Powl J.C., J. Chem. Soc., Faraday Trans. I. 1976, **72** p. 619

[22] Saito A., Foley C., AIChE J. 1991, **37** p. 429

[23] Saito A., Foley C., Microporous Mater. 1995, **3** p. 531

[24] Tarazona P., *Physical Review* **31**, 2672 (1985), Evans, R., Tarazona, P., *Phys. Rev. A*, **31** (1985) 2672; Tarazona, P., Evans, R. Mol. Phys. 1984, **52** p. 847

[25] Seaton N.A., Walton J.R.B., Quirke N., Carbon. 1989, **27** p. 853

[26] LASTOSKIE C.M., GUBBINS K., QUIRKE N., J. Phys. Chem. 1993, **97** p. 4786

[27] OLIVIER J.P., J. Porous Mater. 1995, **2** p. 9

[28] RAVIKOVITCH P., VISHNYAKOV A., NEIMARK A.V., Phys. Rev. E Phys. 2001, **64** p. 011602

[29] LANDERS J., GOR G. Y., A.V. Neimark, Colloids and Surfaces A: Physicochemical and Engineering Aspects **437** (2013) 3-32

[30] KIERLIK E., ROSINBERG M.L., Phys. Rev. A. 1990, **42** p. 3382

[31] ROSENFELD Y., Phys. Rev. Lett. 1989, **63** p. 980

[32] NEIMARK A.V., Langmuir. 1995, **11** p. 4183

[33] RAVIKOVITCH P.I., DOMHNAILL S.C., NEIMARK A.V., SCHUETH F., UNGER K.K., Langmuir. 1995, **11** p. 4765

[34] RAVIKOVITCH P.I., NEIMARK A.V., Langmuir. 2002, **18** p. 1550

[35] SWEATMAN M.B., QUIRKE N., Langmuir. 2001, **17** p. 5011

[36] RAVIKOVITCH P.I., VISHNYAKOV A., RUSSO R., NEIMARK A.V., Langmuir. 2000, **16** p. 2311

[37] NEIMARK A.V., RAVIKOVITCH P.I., Microporous Mesoporous Mater. 2001, **44-45** p. 697

[38] PROVENCHER S.W., Comput. Phys. Commun. 1982, **27** p. 213

[39] WAHBA G., SIAM J. Numer. Anal. 1977, **14** p. 651

[40] LANDERS J., GOR G. Y, NEIMARK A.V., Colloids Surf. A Physicochem. Eng. Asp. 2013, **437** p. 3

[41] JAGIELLO J., OLIVIER J.P., J. Phys. Chem. C. 2009, **113** p. 19382

[42] MIYAHARA M.T., NUMAGUCHI R., HIRATSUKA T., NAKAI K., TANAKA H., Adsorption. 2014, **20** p. 213

[43] ISO 15901-1, *Evaluation of pore size distribution and porosity of solid materials by mercury porosimetry and gas adsorption — Part 1: Mercury porosimetry*

[44] ISO 80000-1, *Quantities and units — Part 1: General*

ICS 19.120

Price based on 29 pages